Relative Contribution of Trabecular and Cortical Bone to Primary Implant Stability: An In Vitro Model Study

Russell Wang, DDS, MSD[1]*
Steven J. Eppell, PhD[2]*
Christian Nguyen, BSc[3]
Nathan Morris, PhD[4]

The specific aim of this study was to examine the relative contributions to the implant insertion torque value (ITV) by cortical and trabecular components of an in vitro bone model. Simulated bone blocks of polyurethane were used with 2 densities of foam (0.08 g/cm^3 to mimic trabecular bone and 0.64 g/cm^3 to mimic cortical bone). We have developed a new platform technology to collect data that enables quantitative evaluation of ITV at different implant locations. Seven groups were used to model varying thicknesses of cortical bone over a lower-quality trabecular bone that have clinical significance: a solid 0.08 g/cm^3 block; 1 mm, 2 mm, and 3 mm thick 0.64 g/cm^3 sheets with no underlayer; and 1 mm, 2 mm, and 3 mm thick 0.64 g/cm^3 sheets laminated on top of a 4 cm thick 0.08 g/cm^3 block. The ITVs were recorded as a function of insertion displacement distance. Relative contributions of ITV ranged from 3% to 18% from trabecular bone, and 62% to 74% from cortical bone depending on the thickness of the cortical layer. Inserting an implant into 2-mm and 3-mm cortical layers laminated atop trabecular blocks had a synergistic effect on ITVs. Finally, an implant with a reverse bevel design near the abutment showed final average torque values that were 14% to 34% less than their maximum torque values. This work provides basic quantitative information for clinicians to understand the influence of composite layers of bone in relation to mechanical torque resistances during implant insertion in order to obtain desired primary implant stability.

Key Words: primary implant stability, insertion torque, implant design, torque-displacement curve, mechanical contribution of cortical bone

INTRODUCTION

Long-term success of dental implants depends on quality of the implant-bone interface.[1–3] Primary implant stability is a prerequisite for implant survival, as it prevents micromovement and subsequent formation of connective tissue layers between implant and bone, thus ensuring bone healing and osseointegration. Biomechanically, 3 factors determine primary implant stability: quality of bone, drilling condition, and implant screw design.

The outer wall of human jawbones consists of a thin cortical layer in the occlusal direction, ranging from 0.5 mm to 2.5 mm.[4–6] Total implant engagement of the cortical bone in the occlusal aspect is often $<$10% of the implant length. Based on this small contact area, it is often assumed that the cortical layer contributes little to the strength of the bone-implant interface. However, there is no qualitative or quantitative information regarding the contribution of overall mechanical strength from trabecular and cortical components of human jawbones. Mechanically, cortical and trabecular layers are significantly different materials. These differences critically impact clinically relevant parameters like resistance to implant insertion torque and final placement torque of implants.

In validation experiments of computer models and in vitro experiments for bone biomechanics and implant testing, human cadaver bone is the material of choice. However, challenges exist in using cadaveric bone to conduct biomechanical experiments, including availability, storage requirements, high cost, possibility of infection, and large variability in sample mechanics. These challenges make synthetic bone analogs an attractive alternative. The uniformity and consistency of rigid polyurethane is ideal for comparative testing of various medical devices and implants. An example for clinically relevant testing can be found in studies of osteoporotic bone. In searching for an in vitro osteoporotic model, mechanical properties of osteoporotic cadaver bone and synthetic bone (Sawbones, Pacific Research Laboratories Inc, Vashon, Wash) made of polyurethane foam with densities of 0.08 g/cm^3 and 0.16 g/cm^3, respectively, were compared. The mechanical

[1] Department of Comprehensive Care, School of Dental Medicine, Case Western Reserve University, Cleveland, Ohio.
[2] Department of Biomedical Engineering, Case School of Engineering, Case Western Reserve University, Cleveland, Ohio.
[3] School of Dental Medicine, Case Western Reserve University, Cleveland, Ohio.
[4] Department of Epidemiology and Biostatistics, School of Medicine, Case Western Reserve University, Cleveland, Ohio.
* *Corresponding authors,* e-mails: rxw26@case.edu; sje@case.edu
DOI: 10.1563/aaid-joi-D-14-00322

TABLE 1

Mechanical properties of polyurethane test block #5 and block #40

Material	Density (g/cm^3)	Compressive		Tensile		Shear	
		Strength (MPa)	Modulus (MPa)	Strength (MPa)	Modulus (MPa)	Strength (MPa)	Modulus (MPa)
Block #5 as underlayer	0.08	0.6	16	1.0	32	0.59	7.1
Block #40 as overlayer	0.64	31	759	19	1000	11	130

fracture properties of the Sawbones and cadaver bone were found to be similar.[6,7]

The specific aim of this work was to study the relative contributions of implant insertion torque values from cortical and trabecular components of an osteoporotic bone model in vitro as a function of implant displacement during insertion. Our hypothesis was that insertion torque values are significantly different from the cortical and trabecular components when inserting dental implants into a jawbone. We also tested and analyzed how variables of implant diameter and thickness of simulated cortical layer affected insertion torque values.

MATERIALS AND METHODS

Simulated bone block construction

Simulated bone blocks of polyurethane rigid foams (Sawbones) were used: 0.08 g/cm^3 to mimic trabecular bone and 0.64 g/cm^3 to mimic cortical bone. Both materials meet ASTM F-1839-08 specifications,[8] and their nominal properties are presented in Table 1. We constructed 7 models of varying thickness of cortical bone (0.64 g/cm^3) over a lower-quality trabecular bone (0.08 g/cm^3): a solid 0.08 g/cm^3 block ~4 cm thick; 1 mm, 2 mm, and 3 mm thick 0.64 g/cm^3 sheets with no underlayer; and 1 mm, 2 mm, and 3 mm thick 0.64 g/cm^3 sheets laminated on top of a 4 cm thick 0.08 g/cm^3 block. To ensure that the thin sheets with no underlayer did not bend during drilling and implant insertion, a low-density block was fabricated with ~1 cm diameter holes drilled in it. We laminated the thin sheets over this block and then did our drilling and implant insertion over the holes.

Implants

Two types of self-tapping titanium implants were used (NobelActive, Nobel Biocare AB, Goteborg, Sweden) for insertion torque tests: narrow platform (NP) 3.5 mm in diameter and regular platform (RP) 4.3 mm in diameter. Both implants are sold as 13 mm-long devices. Actual measured lengths showed the implants to be 12.5 mm long.

Torque vs displacement setup

Samples were tested in a modified commercial torque measurement unit (Figure 1) (MARK-10 Corporation, Copiague, NY). A flat reflective surface (Figure 1d) was attached to a part of the system that translated axially during implant insertion, and was used with a laser displacement sensor (model RS422, Micro-epsilon Inc, Raleigh, NC) to determine axial displacement as a function of time (Figure 1f). An axial compensator provided a uniform dead load, 256 g ± 11 g (N = 8), to drive insertion of

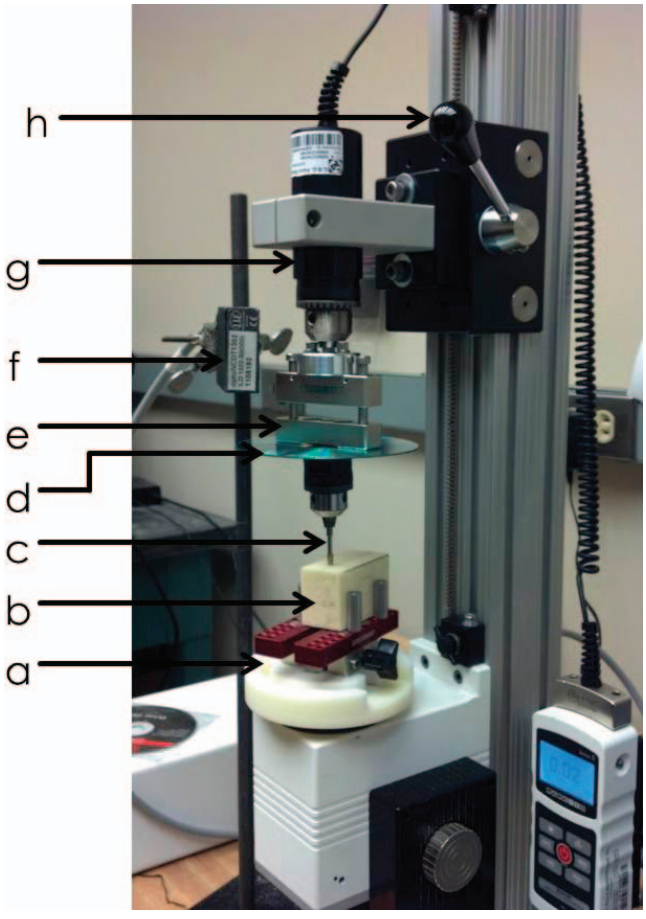

FIGURE 1. Setup used to measure torque vs displacement curves when drilling and placing implants into simulated bone blocks. (a) Custom-made platform that rotates the sample (b) at a pre-set rate. The implant driver (c) is attached to the lower chuck and is shown driving an implant into a sample. A modified compact disc (d) is used as a reflecting surface that moves in lock step with the implant driver. The axial compensator (e) allows the implant driver to move freely up and down while the sample is rotating. The lower bar of the compensator moves while the upper bar remains stationary and transmits the torque felt by the implant to the torque sensor (g) via the upper chuck located between the sensor and the compensator. Displacements are measured using a laser sensor (f) that is fixed in the lab frame by a ring stand and probes the position of the reflecting surface. The implant is initially brought into contact with the sample and the lower bar of the compensator raised to nearly touch the upper bar using the axial actuator handle (h).

TABLE 2

Summary of means and standard deviations of final insertion torque values for all groups*

Implant Type	Overlayer Thickness	Block #5	N	Mean Final Torque (N-cm)	P
RP	0	Y	30	3.8 ± 0.9	
RP†	1 mm	Y	18	21.5 ± 4.4	9.1×10^{-9}
RP†	2 mm	Y	11	48.6 ± 3.9	9.4×10^{-6}
RP†	3 mm	Y	7	88.2 ± 3.8	6.3×10^{-5}
RP†	1 mm	N	8	14.5 ± 3.9	1.8×10^{-5}
RP†	2 mm	N	10	34.7 ± 5.2	4.6×10^{-5}
RP†	3 mm	N	15	65.2 ± 3.8	3.6×10^{-5}
NP	0	Y	8	1.7 ± 0.5	
NP†	1 mm	Y	6	11.1 ± 0.6	6.7×10^{-4}
NP	2 mm	Y	5	33.7 ± 2.2	4.3×10^{-3}
NP†	3 mm	Y	8	54.7 ± 2.5	1.6×10^{-3}
NP†	1 mm	N	12	7.8 ± 2.7	2.3×10^{-4}
NP†	2 mm	N	8	16.3 ± 1.6	2.5×10^{-4}
NP†	3 mm	N	13	33.8 ± 6.9	1.9×10^{-4}

*Implant types tested were regular platform (RP) and narrow platform (NP). Overlayer thicknesses ranged from 0 to 3 mm. The block column indicates whether the test was made with overlayers laminated to an underlying low-density block (Y) or with overlayers over an air-filled space (N). Results are presented in ascending order of overlayer thickness for each implant type and underlayer condition. A Wilcoxen rank-sum test was used to test if increasing overlayer thickness produced a statistically significant increase in final torque compared with the next lowest thickness. The 1-mm overlayer cases were tested against the zero overlayer case for their respective implant types. A dagger (†) in column 1 indicates that the particular row had a statistically significantly higher final torque using a Bonferroni corrected cutoff of $\alpha = 0.05/32$, where 32 is the total number of comparisons made throughout this study.

TABLE 3

Mean falloff from maximum insertion torque to final torque

Implant Type	Overlayer Thickness (mm)	Block	Mean Falloff (N-cm)	Mean Falloff (%)	P
RP†	0	Y	−1.2 ± 0.34	0 ± 1	3.4×10^{-4}
RP†	1 mm	Y	20.9 ± 5.0	49 ± 11	$<1 \times 10^{-6}$
RP†	2 mm	Y	18.2 ± 4.2	27 ± 6	$<1 \times 10^{-6}$
RP	3 mm	Y	17.7 ± 3.7	17 ± 3	2.3×10^{-3}
RP†	1 mm	N	13.9 ± 4.0	49 ± 14	5.8×10^{-4}
RP†	2 mm	N	24.5 ± 5.3	41 ± 9	1.1×10^{-4}
RP†	3 mm	N	18.2 ± 4.5	22 ± 5	$<1 \times 10^{-6}$
NP†	0	Y	−1.0 ± 0.4	1 ± 2	$<1 \times 10^{-6}$
NP	1 mm	Y	0.1 ± 0.2	1 ± 2	1.6×10^{-2}
NP	2 mm	Y	4.6 ± 1.5	9 ± 3	0.63
NP	3 mm	Y	3.0 ± 2.5	5 ± 4	7.1×10^{-3}
NP	1 mm	N	1.7 ± 1.0	17 ± 10	9.4×10^{-3}
NP	2 mm	N	0.6 ± 0.3	3 ± 2	9.4×10^{-3}
NP	3 mm	N	0.4 ± 0.9	1 ± 2	3.7×10^{-3}

*Implant types tested were regular platform (RP) and narrow platform (NP). Overlayer thicknesses ranged from 0 to 3 mm. The block column indicates whether the test was made with overlayers laminated to an underlying low-density block (Y) or with overlayers over an air-filled space (N). The mean falloff is the drop from maximum torque to final torque and is reported in both N-cm and as a percent of the maximum torque. Because the maximum torque is guaranteed to be greater than or equal to the final torque, statistical significance of the dropoff was calculated between the torque at an axial displacement of 10.5 mm and the final torque (Table 2) using the Wilcoxon signed-rank test for paired data. A dagger (†) in column 1 indicates that the particular row had a statistically significant falloff from maximum to final torque using a Bonferroni corrected cutoff of $\alpha = 0.05/32 = 1.6 \times 10^{-3}$, where 32 is the total number of comparisons made throughout this study.

implants (Figure 1e). A torque sensor (Model M7-500, MARK-10 Corporation) was used to record torque as a function of time.

Implant procedure

Manufacturer-recommended protocols for surgical placement of implants were followed. The Sawbones model material provided good mechanical reproducibility for comparison purposes among implants. Drill sequences across all 7 models were standardized with final drills of 2.8/3.2 mm diameter for NP implants and 3.2/3.6 mm for RP implants. These are manufacturer recommended final drill sizes for placement into dense cortical bone. Since the 3-mm overlayers required the dense bone protocol, we decided to use the same drill sizes for all the other samples to eliminate drill diameter as a variable in this study. Implants were aligned with a predrilled hole; the sample was rotated at 1 Hz; recording of torque and axial displacement at 1-millisecond intervals was started; and the axial actuator handle (Figure 1h) was used to move the implant down until the compensator dead load was applied. Insertion was stopped when the top of the implant was flush with the surface of the test piece. Each combination of Sawbones block, drill size, and implant type was tested multiple times ($5 \leq N \leq 30$)

Analysis of data

Torque vs axial displacement curves were plotted and used to obtain means and standard deviations of maximum torque, final torque, and dropoff between maximum and final torque. All values are reported as means ± standard deviations. The difference between groups in Table 2 was determined using the Wilcoxon rank-sum (2-sample) test. Because the maximum torque is guaranteed to be greater than or equal to the final torque, statistical significance of the dropoff between the torque at an axial displacement of 10.5 mm and the final torque (Table 3) was calculated using both the Wilcoxon signed-rank test for paired data and studentized bootstrap resampling.[9,10] The *P* values reported in Table 3 were computed by the bootstrap analysis. The data summarized in Table 4 required a test statistic that included 3 means and 3 variances, and so was not amenable to a nonparametric test. For this analysis, we used a *t*-like statistic with

$$t = [\overline{UO} - (\overline{O} + \overline{U})] / \sqrt{\frac{S_{OU}^2}{n_{OU}} + \frac{S_O^2}{n_O} + \frac{S_U^2}{n_U}}$$

along with studentized bootstrap resampling[9,10] to perform a 2-tailed test that disproved the hypothesis that there was no synergy, and to estimated the amount of synergy. Here, $\overline{UO}$, $\overline{U}$, and $\overline{O}$ represent the sample mean of the samples with under/over layer, just the under layer, and just the over layer, respectively, while S_{OU}^2, S_U^2, S_O^2, n_{OU}, n_U, and n_O are the respective sample variances and sample sizes. Finally, the family-wise error rate was controlled for using the conservative Bonferroni correction. Statistical significance was assigned with $\alpha = 0.05/32$

TABLE 4

Relative contribution of insertion torque value from simulated trabecular bone and 3 thickness of cortical bone overlayer*

		1 mm Thick Cortical Overlayer				2 mm Thick Cortical Overlayer				3 mm Thick Cortical Overlayer			
	U	O	U&O	Syn	*P*	O	U&O	Syn	*P*	O	U&O	Syn	*P*
RP	4	14	22	4	.09	35	49	10	4.6×10^{-5}†	65	88	19	1.1×10^{-6}†
NP	2	8	11	1	.09	16	37	19	1.6×10^{-5}†	34	55	19	7.0×10^{-6}†

*U indicates underlayer alone; O, overlayer alone; U&O, combination of underlayer and overlayer; RP, regular platform implant; NP, narrow platform implant; Syn, the synergistic excess of the laminated U&O sample over the sum of the components of the laminate measured separately (U + O). All numbers are reported in Ncm. The *P* values for a synergistic effect shown in the *P*. A dagger (†) next to the *P* value indicates that the *P* value is statistically significant even after using a conservative Bonferroni corrected cutoff of $\alpha = 0.05/32$, where 32 is the total number of comparisons made throughout this study.

≈ 0.0016. Here, 32 is the total number of comparisons made throughout the study: 12 in Table 2, 14 in Table 3, and 6 in Table 4.

RESULTS

All torque vs displacement plots shown below are averages of multiple curves. Figure 2 shows a typical situation, Figure 2a shows 18 individual curves, and Figure 2b shows a single curve representing the average of these 18 curves with error bars indicating standard deviations of the individual curves about the mean. Table 2 summarizes all the conditions tested giving means and standard deviations of final insertion torques for each group. The following sections present the three main findings of this study.

Regular platform implants can have a final insertion torque less than the maximum torque

Figure 3 shows torque vs displacement curves for implants inserted into a 1-mm simulated cortical bone layer laminated atop a thick simulated trabecular block. The regular platform implant peak occurs near 10.5-mm axial displacement and is ~20 N-cm higher than the torque at final placement near 12.5 mm. This falloff is absent with narrow platform implants, which show monotonic increase to maximum torque (Figure 3, lower curve). In addition, this falloff is absent with regular platform implants inserted into homogenous samples (see, for example, the monotonically increasing curve, Figure 3 inset). Table 3 shows mean falloffs for all tested groups. The RP and NP implants were inserted into overlayers of 1 mm to 3 mm thickness. These overlayers either had a low-density block beneath them (Y) or an air-fill space beneath them (N). Implants placed into low-density blocks with no overlayer show a zero in the overlayer thickness column. Mean falloffs, computed as the difference between the maximum insertion torque and the final torque, are reported in both N-cm and percentage of maximum torque where ± corresponds to standard deviation. This is an accurate reflection of what the data looks like for curves, such as those shown in Figure 2. However, statistical significance is not robustly calculable using this measurement because the value is guaranteed to be nonnegative. For this reason, to

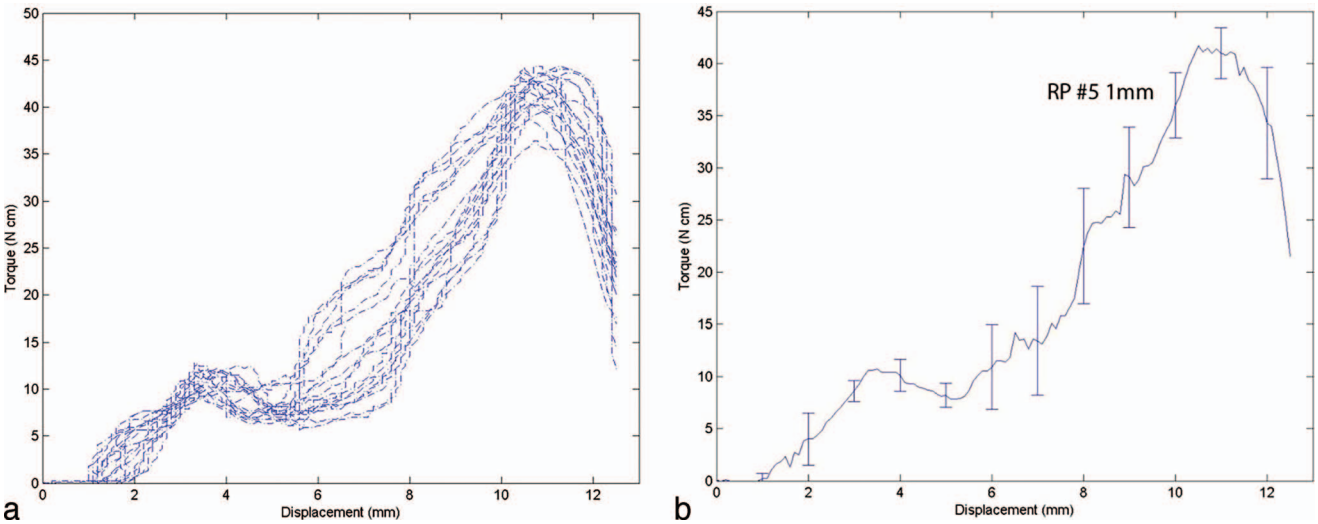

FIGURE 2. Multiple torque vs displacement curves were taken for every combination of implant type (regular platform and narrow platform) and every sample condition (simulated trabecular bone, simulated cortical bone of varying thicknesses, and simulated thin cortical bone overlayers affixed atop simulated trabecular bone). (a) Example showing 18 torque vs displacement curves using a regular platform (RP) implant being inserted into a 1-mm-thick dense cortical overlayer (#40 Sawbones) fixed atop a thick simulated trabecular underlayer (#5 Sawbones). To visualize multiple different conditions on the same plot, we simplified the presentation of these data by plotting the mean torque value at each displacement to obtain 1 curve from the multiple runs. (b) Standard deviation bars indicate the distribution of the data about this mean.

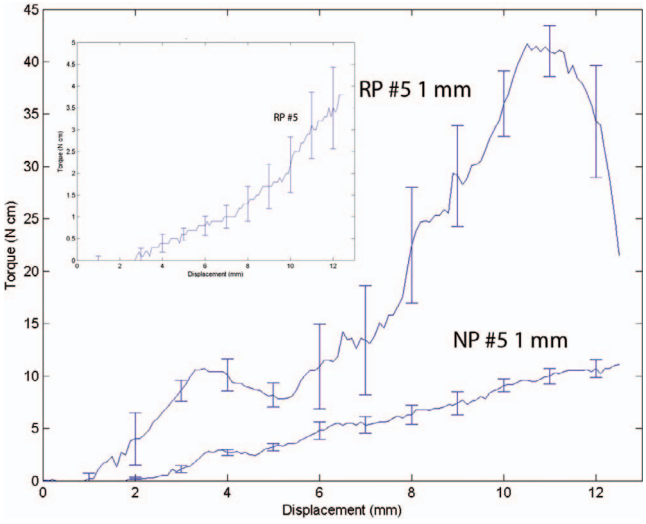

Figure 3. The regular platform (RP) implants showed a distinct drop in insertion torque in the last few millimeters of travel when being inserted into a dense cortical overlayer affixed atop a low-density trabecular underlayer. The narrow platform implants showed no such drop. This figure shows data for a 1-mm-thick #40 (dense/cortical) Sawbones overlayer affixed atop a #5 (low-density/trabecular) Sawbones underlayer. The inset shows the RP implant being placed into a pure low-density trabecular layer showing no drop in torque. The effect is thus due to the thin dense cortical overlayer. NP indicates narrow platform.

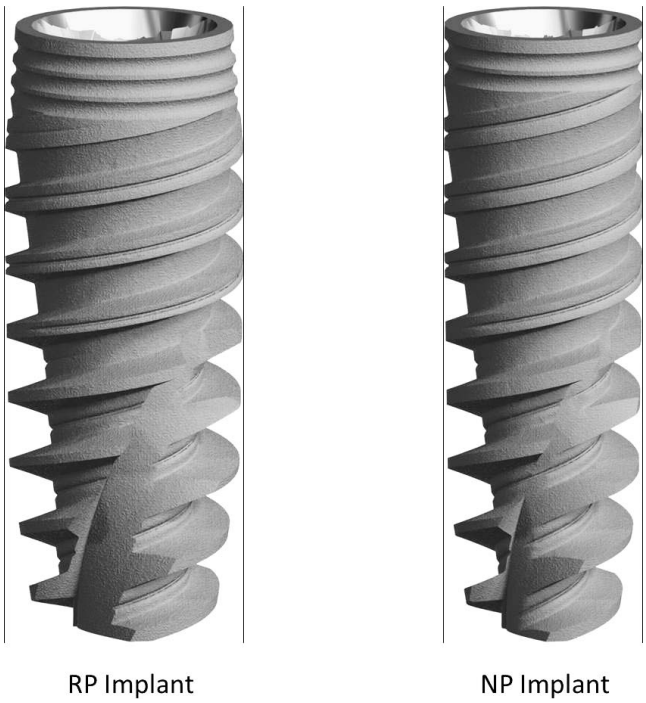

Figure 4. Images of the 2 implant types used in this study: Nobel Biocare regular platform (RP) and narrow platform (NP). The RP implant has a retrograde slope near the top of the implant while the NP implant does not. In addition, the thread patterns are clearly complex, which adds structure to the torque vs displacement data not typical of a more simply threaded screw.

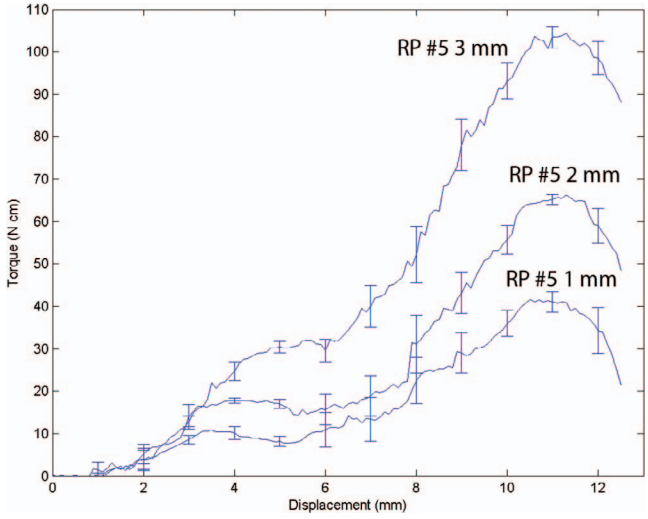

Figure 5. Increasingly thick dense cortical overlayers atop low-density trabecular underlayers resulted in increasing values of insertion torque. The overall magnitude of the drop in insertion torque consistently occurred near the same value of insertion displacement, consistent with this drop being the result of the geometric design of the implant. In addition, the magnitude of the drop in insertion torque remained constant as the overlayer thickness increased. RP indicates regular platform.

compute *P* values, we used the insertion torque at 10.5 mm. This is the displacement at which the retrograde slope of the RP implants just began to insert into the samples (see, for example, Figure 4). Statistically significant falloffs ($P < .05/32$, where 32 is the total number of tests in this article) have a dagger in the *P* column. Implants placed into low-density blocks with no overlayer (rows 1 and 8 in Table 3) showed no falloff. These curves simply rose until the final value, similar to all the NP implants. Thus, these rows show a statistically significant difference between 10.5 mm and the final torques at 12.5 mm. However, this difference was not a falloff, it was a rise to the final torque. There was one outlier with respect to statistical significance: the RP implant with a 3-mm overlayer atop a low-density underlayer (row 4 in Table 3). This condition did not show a statistically significant falloff at the Bonferroni corrected alpha value of 0.0016 using the bootstrap analysis. This particular case had a small sample size of 7. In addition, the Wilcoxen signed rank test did show this case to be significant with a *P* value of 6.3×10^{-5}. The average falloff for RP implants was 34% ± 14%. The average falloff for the NP implants was 6% ± 6%.

Thickness of cortical overlayer between 1 and 3 mm affects insertion torque

Figure 5 shows torque vs axial displacement curves for a regular platform implant placed into layered constructs having 1–3 mm dense overlayers laminated on top of a low-density block. The general curve shape is similar to that shown in Figure 3. After 3 mm of axial insertion, torque as a function of axial insertion distance clearly increases with overlayer thickness. The drop in torque from its maximum value to the final position of the implant is ~19 N-cm and does not change much as a function

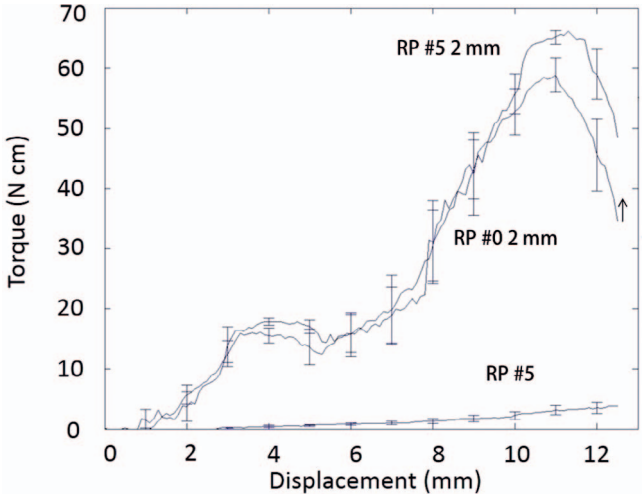

Figure 6. A synergistic effect occurs when inserting implants into thin dense overlayers atop lower-density underlayers. For example, looking at the final insertion torques, the underlayer alone (regular platform [RP] #5, 3.8 N-cm) plus the overlayer alone (RP #0 2 mm, 35 N-cm) is only 71% of the final torque measured when inserting the implant into the combined layers (RP #5 2 mm, 49 N-cm). The small arrow to the right of the (RP #0 2 mm) curve shows the additional torque from the underlayer alone. The distance along the torque axis from the tip of the arrow to the (RP #5 2 mm) curve represents the synergistic effect.

of overlayer thickness. Table 2 is organized in order of increasing overlayer thickness for each implant type (NP and RP), and each condition of having a low-density underlayer or not (Y and N). For each group, the mean final torque values clearly increase with increasing overlayer thickness. Statistical significance of this was determined using a Wilcoxon rank-sum test. Similar results were also obtained using a Welch's *t*-test (data not shown). All but one of the rows (the NP 2-mm overlayer with underlayer present) showed a statistically significantly higher mean final torque compared with the row above. This one condition likely failed to show statistical significance because both the 1-mm and 2-mm measures in this group had a small number of measurements.

The synergistic increase in final torque is due to the low-density underlayer

Figure 6 shows torque vs displacement curves for a regular platform implant inserted into 3 different constructs. Insertion into a pure low-density block #5 shows a final insertion torque of 3.8 ± 0.9 N-cm (bottom curve). Insertion into a 2-mm-thick overlayer supported over an air-filled space shows a final insertion torque of 34.7 ± 5.2 N-cm (middle curve). Insertion into a 2-mm-thick overlayer laminated on top of a low-density block shows a final insertion torque of 48.6 ± 3.9 N-cm (top curve). The sum of final torques into the 2 elements taken alone was 38.5 N-cm (indicated by the top of the vertical arrow shown near the end of the middle curve in Figure 6) or 10.1 N-cm less than the final torque into the laminated construct.

Table 4 summarizes relative contributions of final insertion torque values from simulated trabecular bone underlayers (U) and 3 thicknesses of cortical bone overlayers (O). The numbers are reported in N-cm. In every case, the final torque of the laminated construct is greater than the sum of the individual components of the laminate measured separately. In addition, scanning across each row, the magnitude of this synergistic effect due to layering increases with overlayer thickness. A bootstrap resampling approach[9,10] showed that synergistic increase in final torque exists for both NP and RP implants placed into constructs having 2 mm or 3 mm thick overlayers. In these cases, the *P* values for a 2-tailed test (Table 4) were much smaller than the Bonferroni corrected alpha level. Constructs with 1-mm overlayers did not show a similar strong effect and had *P* values of .09.

Discussion

The measurement system developed for this study allows for quantitative evaluation of primary implant stability for different implant designs. Most published studies on insertion torque of dental implants are based on final insertion torque generated by a manual torque wrench.[11–22] The manual torque method gives clinicians only 1 data point during implant insertion. Other studies use torque vs time data to study primary implant stability. While providing more information than the single-point final insertion torque method, using time as the independent variable is problematic. The rate at which implants progress into samples varies for multiple reasons, including the amount of manual compressive loading forces applied by clinicians, complexity of implant thread design, uncontrollable fracture of bone and bonelike synthetic materials leading to rapid advancement of the implant, and inhomogeneity in the sample material causing occasional slippage at the implant-sample interface resulting in rotation of the implant without subsequent axial advancement. In contrast, plots of insertion torque vs axial displacement, as presented in this study, allow for characterization and quantification of mechanical behavior at any location of an implant during insertion. This allows for a kind of "mechanical spectroscopy" where the shape of the torque vs displacement curve correlates with the physical situation during the insertion process.

A rudimentary example of this mechanical spectroscopy is seen in data showing RP implants having final insertion torques less than the maximum torque. Final torques are assumed to be the maximum torques in many published studies. Our data show this assumption can be incorrect if there is a reversed bevel at the top of an implant. Figure 4 shows that RP implants have a retrograde slope near the top. Our study shows this back-tapered coronal design compromises mechanical strength during implant insertion. The drop-off from maximum to final torque ranged from 17% to 49% (rows 2–7 in Table 3) depending on the cortical bone construct. The average drop-off of all conditions is 34%, excluding the trabecular block alone for the RP implant groups. The NP implant lacks this retrograde slope and does not show the falloff in torque during insertion. In addition to this drop in torque, the complex thread design shows up in the data as 1 or 2 plateaus between 3 and 8 mm as well as several smaller features in the curves. This may provide a structure-function link between implant design and mechanics of implantation.

In addition to providing mechanics related to geometry,

the measurement system provides automated, reproducible quantitative measures of implant behavior. For example, Table 4 shows the percentage of total final insertion torque contributed from the trabecular underlayer component clearly decreasing as thickness of the cortical overlayer increases. The final insertion torque of an RP implant inserted into a 1-mm-thick cortical overlayer showed a contribution from the trabecular component of 18%. This is remarkable given that 92% of the surface contact between implant and sample was accounted for by this trabecular underlayer. Once the cortical layer reached 3 mm for the RP implant, the trabecular component contributed only 5% to the final insertion torque, an almost negligible quantity. Clinical significance of this result rests on the fact that human bones are anisotropic layered composite materials exhibiting a great variation of their mechanical properties. The moduli of cortical bone ranges from 8.6 to 25.9 GPa and of trabecular bone from 4.3 to 6.8 GPa.[23–25] Tables 2 and 3 provide quantitative measures demonstrating the important contribution of a cortical layer to the overall final insertion torque. This correlates with primary implant stability. Therefore, for a patient with osteoporosis, the layer of cortical bone may be the key factor for a clinician to be able to predict potential risks or successes of obtaining an acceptable final insertion torque necessary for primary implant stability.

A secondary but significant effect to cortical layer thickness is seen in Table 4. A statistically significant increase ($P < .05/32$) in final insertion torque is seen with 2-mm and 3-mm cortical layers when the low-density underlayer is present beneath the cortical layer. Even though the underlayer taken alone accounts for $<$10% of the final insertion torque, there is an increase of 14%–47% in overall final insertion torque when the underlayer is present beneath the cortical overlayer. Thus, even though final insertion torque is dominated by the thin cortical overlayer, it is clinically important to pay attention to the lower-quality bone beneath this layer. The difference between fluid-filled space vs low-quality trabecular bone space can impact the final insertion torque by as much as 47%.

The synergistic effect may be explained by considering that when an implant is rotated into a predrilled hole, elastic and plastic deformation of the bone material occurs and forms crack openings as the implant advances. Crack-opening stress is often higher when the crack advances in the wake of plastically deformed materials; eventually, some of the material is sheared off and compressed between threads and bone. Insertion torque is measured from the combined resistance of friction, shear, and compression stresses of trabecular and cortical bone materials at the implant-bone interface. Smear effects and cavity expansion phenomena could explain the observed synergistic effect[26,27]; the final insertion torque into layered constructs is larger than the summation of final insertion torque into overlayer alone plus underlayer alone. The fact that this effect was not strongly apparent with 1-mm overlayers was likely due to the fact that the standard deviations for the 1-mm samples were substantially larger as a percentage of mean torque than their 2-mm and 3-mm counterparts. This likely occurred because these thin overlayers bowed under the axial insertion pressure, causing fluctuations in the measured torques.

The falloff and synergistic effect phenomena observed in this study are intriguing. Torque vs displacement data allow for a better understanding of the characteristics of insertion torque as a function of implant displacement. Results from this in vitro model provide a good foundation for future animal-model studies. Ultimately, information derived from this and future work will be beneficial for clinicians to improve primary implant stability.

Conclusions

A new measurement system was presented enabling quantitative evaluation of insertion torque at different implant locations. The system showed that retrograde slopes negatively impact primary implant stability when inserting into thin dense cortical layers. For Nobel Biocare Regular and NP implants, final torque values depend primarily on the thickness of cortical bone when this layer is 1–3 mm thick. Finally, there is a synergistic effect when inserting implants into thin dense layers over lower-density blocks. The sum of the final insertion torque into the 2 elements taken alone is less than the final torque into the laminated construct.

Abbreviations

NP: narrow platform
RP: regular platform

Acknowledgments

This study received financial support from the American Academy of Implant Dentistry Research Foundation, and Nobel Biocare Services AG provided components (research grant 2011-1050).

References

1. Adell R, Lekholm U, Rockler B, Branemark PI. A 15-year study of osseointegrated implants in the treatment of the edentulous jaw. *Int J Oral Surg*. 1981;10:387–416.

2. Albrektsson T, Branemark PI, Hansson HA, Lindstrom J. Osseointegrated titanium implants. Requirements for ensuring a long-lasting, direct bone-to-implant anchorage in man. *Acta Orthop Scand*. 1981;52:155–170.

3. Zarb GA, Schmitt A. The longitudinal clinical effectiveness of osseointegrated dental implants: the Toronto study. Part III: problems and complications encountered. *J Prosthet Dent*. 1990;64:185–194.

4. Baumgaertel S. Quantitative investigation of palatal bone depth and cortical bone thickness for mini-implant in adults. *Am J Orthod Dentofacial Orthop*. 2009;136:104–108.

5. Wang R, Huang Y, Fan J, Lang L. Quantification of edentulous jaw bones using cone-beam computed tomography (CBCT) images. *J Dent Res*. 2012;91A:1436.

6. Katranji A, Misch K, Wang HL. Cortical bone thickness in dentate and edentulous human cadavers. *J Periodontol*. 2007;78:874–878.

7. Seebeck J, Goldhahn J, Morlock MM, Schneider E. Mechanical behavior of screws in normal and osteoporotic bone. *Osteoporos Int*. 2005; 16(suppl 2):S107–S111.

8. ASTM F1839-08: standard specification for rigid polyurethane foam for use as a standard material for testing orthopedic devices and instruments. In: *ASTM Annual Book of ASTM Standards*. West Conshohocken, PA: ASTM International; 2008. DOI: 10.1520/F1839-08R12.

9. Janssen A, Pauls KT. A Monte Carlo comparison of studentized

bootstrap and permutation tests for heteroscedastic two-sample problems. *Comput Stat*. 2005;20:369–383.

10. Efron B. Bootstrap methods: another look at the jackknife. *Ann Stat*. 1979;7:1–26.

11. Cehreli MC, Kokat AM, Comert A, Akkocaoglu M, Tekdemir I, Akca K. Implant stability and bone density: assessment of correlation in fresh cadavers using conventional and osteotome implant sockets. *Clin Oral Implants Res*. 2010;20:1163–1169.

12. Lee S, Gantes B, Riggs M, Crigger M. Bone density assessments of dental implant sites: bone quality evaluation during osteotomy and implant placement. *Int J Oral Maxillofac Implants*. 2007;22:208–212.

13. Miyamoto I, Tsuboi Y, Wada E, Suwa H, Iizuka T. Influence of cortical bone thickness and implant length on implant stability at the time of surgery—clinical, prospective, biomechanical, and imaging study. *Bone*. 2005;37:776–780.

14. Motoyoshi M, Yoshida T, Ono A, Shimizu N. Effect of cortical bone thickness and implant placement torque on stability of orthodontic mini-implants. *Int J Oral Maxillofac Implants*. 2007;22:779–784.

15. O'Sullivan D, Sennerby L, Jagger D, Meredith N. A comparison of two methods of enhancing implant primary stability. *Clin Oral Implants Res*. 2004;6:48–57.

16. Turkyilmaz I, Tumer C, Ozbek EN, Tozum TF. Relations between the bone density values from computerized tomography and implant stability parameters: a clinical study of 230 regular platform implants. *J Clin Periodontol*. 2007;34:716–722.

17. Alsaadi G, Quirynen M, Michiels K, Jacobs R, van Steenberghe D. A biomechanical assessment of the relation between the oral implant stability at insertion and subjective bone quality assessment. *J Clin Periodontol*. 2007; 34:359–366.

18. Atsumi M, Park SH, Wang HL. Methods used to assess implant stability: current status. *Int J Oral Maxillofac Implants*. 2007;22:743–754.

19. Beer A, Gahleitner A, Holm A, Tschabitscher M, Homolka P. Correlation of insertion torques with bone mineral density from dental quantitative CT in the mandible. *Clin Oral Implants Res*. 2003;14:616–620.

20. Lioubavina-Hack N, Lang NP, Karring T. Significance of primary stability for osseointegration of dental implants. *Clin Oral Implants Res*. 2006; 17:244–250.

21. Tabassum A, Meijer GJ, Wolke JG, Jansen JA. Influence of surgical technique and surface roughness on the primary stability of an implant in artificial bone with different cortical thickness: a laboratory study. *Clin Oral Implants Res*. 2010;21:213–220.

22. Ottoni JM, Oliveira ZF, Mansini R, Cabral AM. Correlation between placement torque and survival of single-tooth implants. *Int J Oral Maxillofac Implants*. 2005;20:769–776.

23. Tamatsu Y, Kaimoto K, Ide A, Ide Y. Properties of the elastic modulus from buccal compact bone of human mandible. *Bull Tokyo Dent Coll*. 1996;37:93–101.

24. Reilly DT, Burstein AH, Frankel VH. The elastic modulus for bone. *J Biomechanics*. 1974;7:271–275.

25. Lettry S, Seedhom B, Berry B, Cupponea M. Quality assessment of the cortical bone of the human mandible. *Bone*. 2003;32:35–44.

26. Salgado R, Randolph M. Analysis of cavity expansion in sand. *Int J Geomechanics*. 2001;2:175–192.

27. Yu Hs, Rowe RK. Plasticity solutions for soil behavior around contracting cavity and tunnels. *Int J Numer Anal Methods Geomech*. 1999;23: 1245–1279.